Supplementary material

Assessing the formation of cobalt carbide and its catalytic performance under realistic reaction conditions and tuning product selectivity in cobalt-based FTS reaction

*Qiang Lin, Bing Liu, Feng Jiang, Xuejin Fang, Yuebing Xu, Xiaohao Liu**

Department of Chemical Engineering, School of Chemical and Material Engineering, Jiangnan University, Wuxi 214122, China

E-mail address: liuxh@jiangnan.edu.cn (X.H. Liu)

Supplementary Figures and Tables

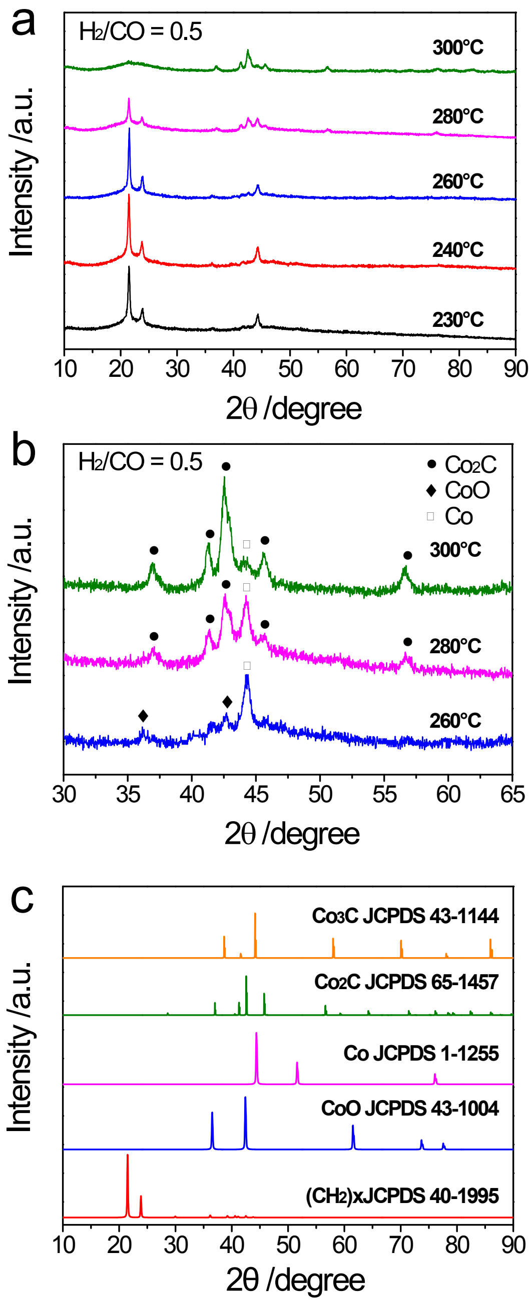

Figure S1 XRD patterns of spent $20Co/SiO_2$ in FTS reaction over different reaction temperatures.

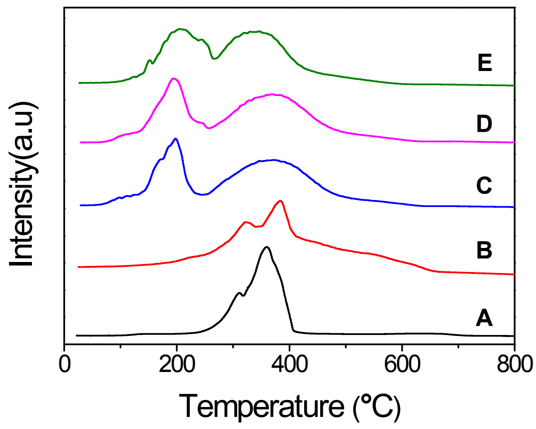

Figure S2 H_2-TPR profiles for 20Co/SiO_2 (A), 20Co5Mn/SiO_2 (B), and Ru-promoted 20Co5Mn/SiO_2 with 0.5wt% (C), 1.0wt% (D), and 2.5wt% Ru (E).

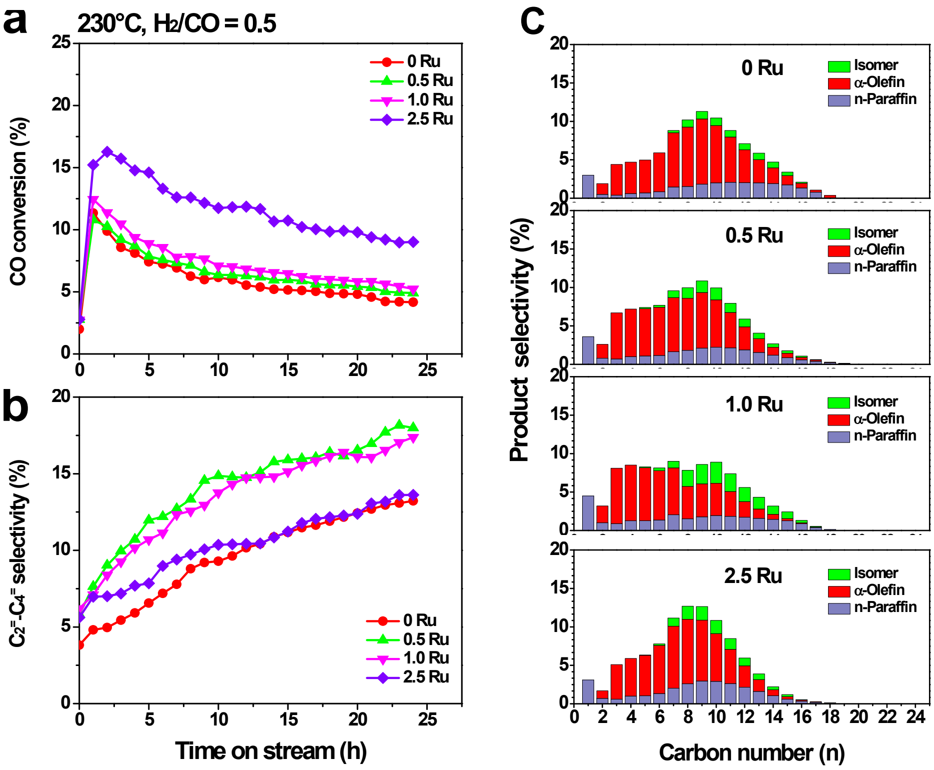

Figure S3 Influence of the Ru loading on CO conversion (a) and $C_2^=$-$C_4^=$ selectivity (b), and carbon number distribution (c) with TOS over 20Co5Mn/SiO_2 catalysts at H_2/CO = 0.5.

As shown in Fig. S3, the Ru promoter indicated the obviously enhanced catalytic activity as the initial CO conversion was higher with the addition of Ru from 0.5% to 2.5 wt.%. The initially higher activity might be ascribed to the improved reduction degree of cobalt oxides or the Ru acting as the FTS component or the enhanced H spillover over catalyst surface. However, the trend for the catalytic activity and the product selectivity has almost not been changed with TOS (Fig. S3b and Fig. S6f), which suggested that the evolution behavior for existing state of cobalt and surface C* species accumulation did not obviously alter with the presence of Ru. The role of Ru was suppressed due to the low H_2 concentration in feed gas.

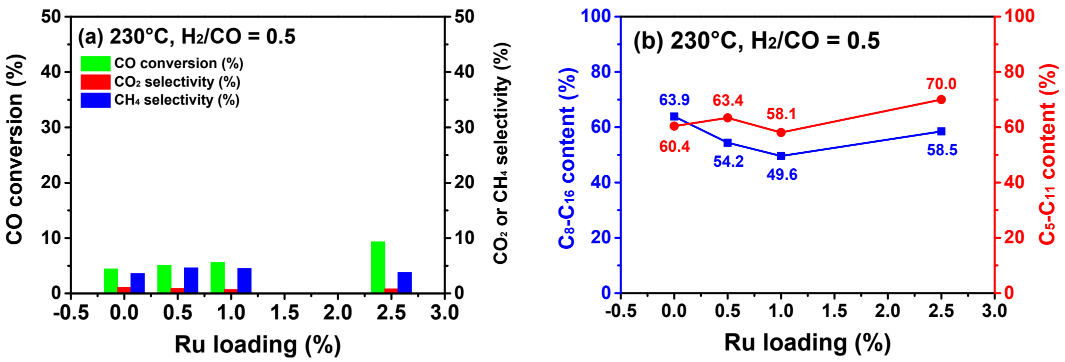

Figure S4 Influence of the Ru loading on CO conversion, CO_2 or CH_4 selectivity (a), and C_8-C_{16} and C_5-C_{11} selectivity (b) over 20Co5Mn/SiO_2 catalyst.

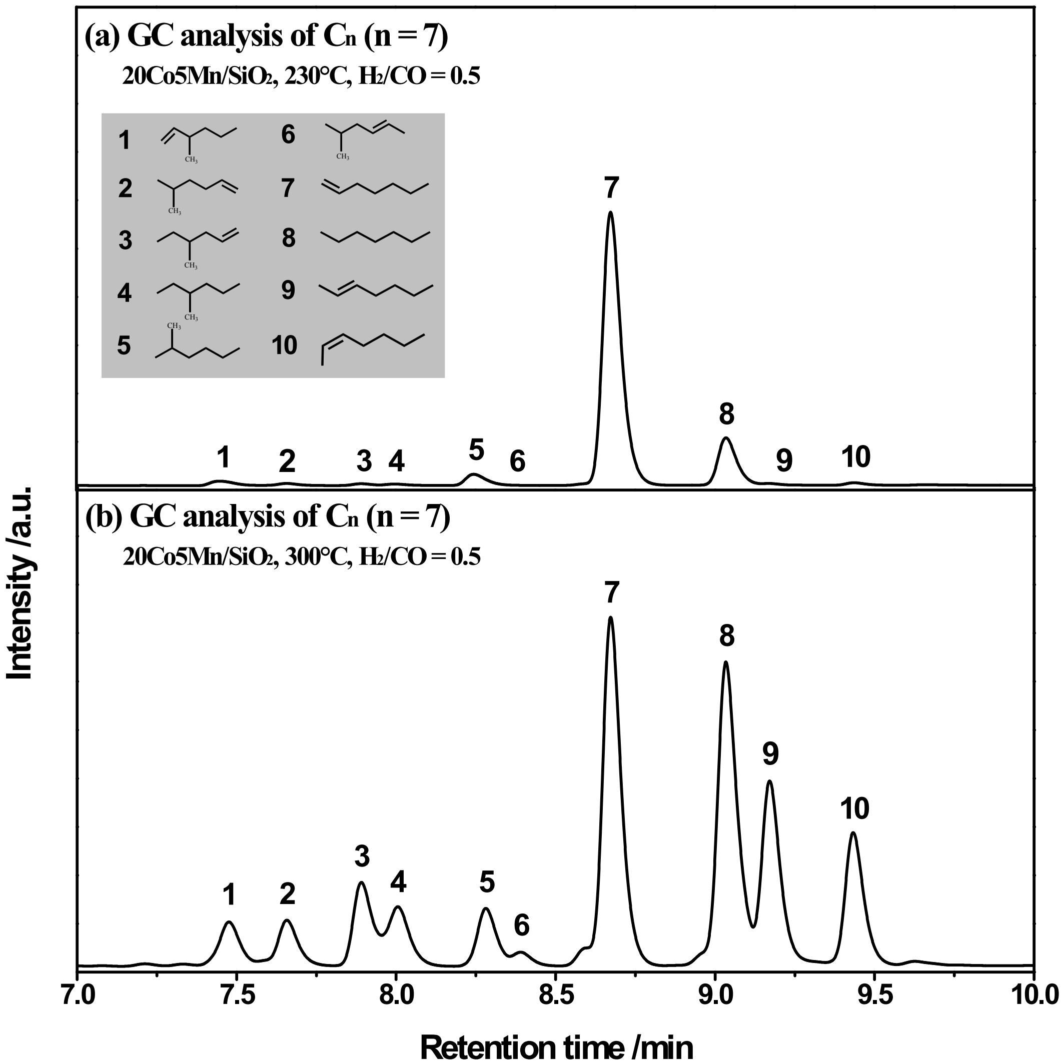

Figure S5 Influence of the reaction temperature on the formation of iso-hydrocarbons over 20Co5Mn/SiO_2 catalyst at H_2/CO = 0.5.

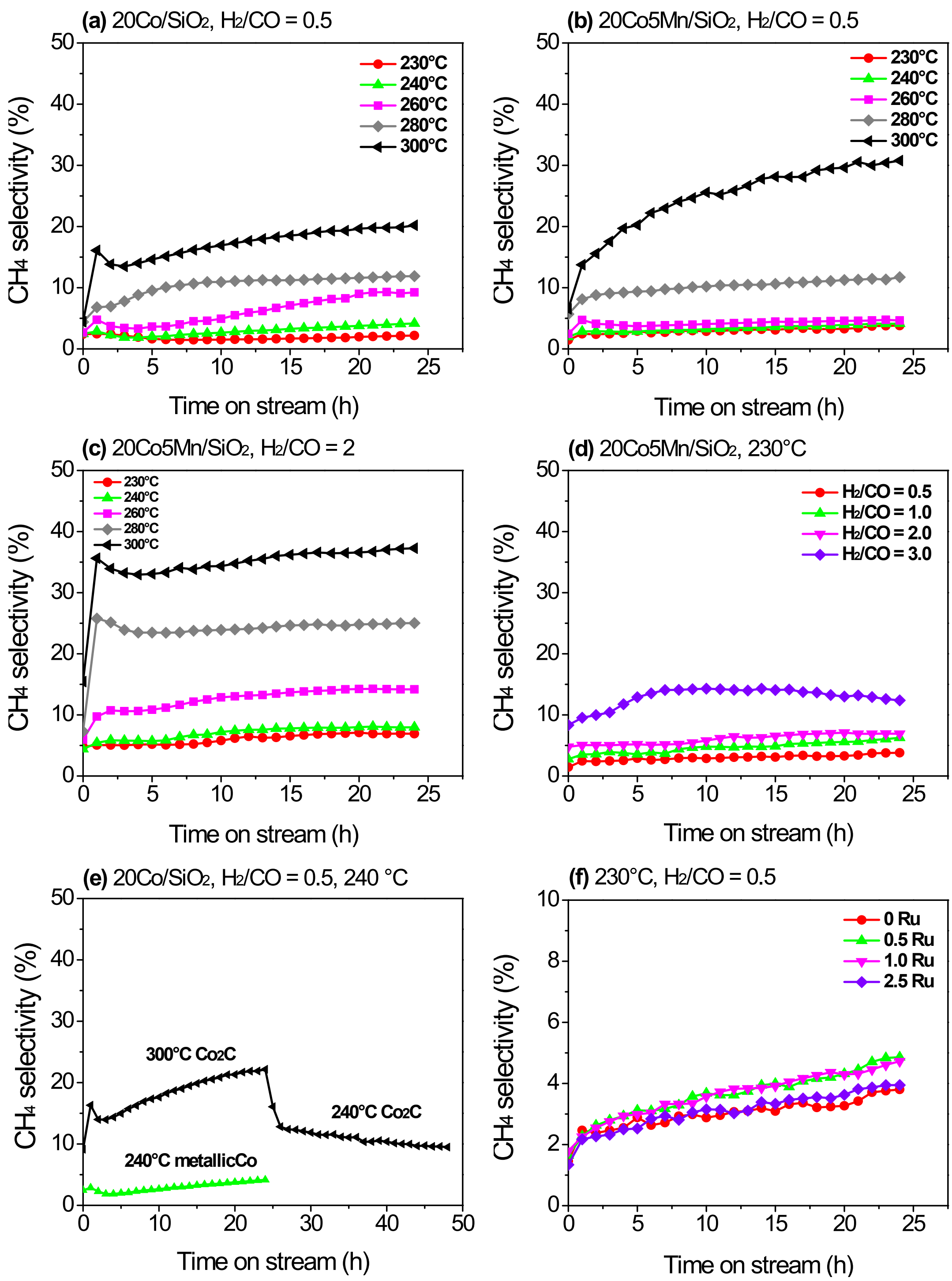

Figure S6 The methane selectivity with TOS under different catalysts and reaction conditions: (a) corresponding to CO conversion in Fig. 7; (b) for that in Fig. 10; (c) for that in Fig. 11; (d) for that in Fig. 12; (e) for that in Fig. 13; (f) for that in Fig. S3.

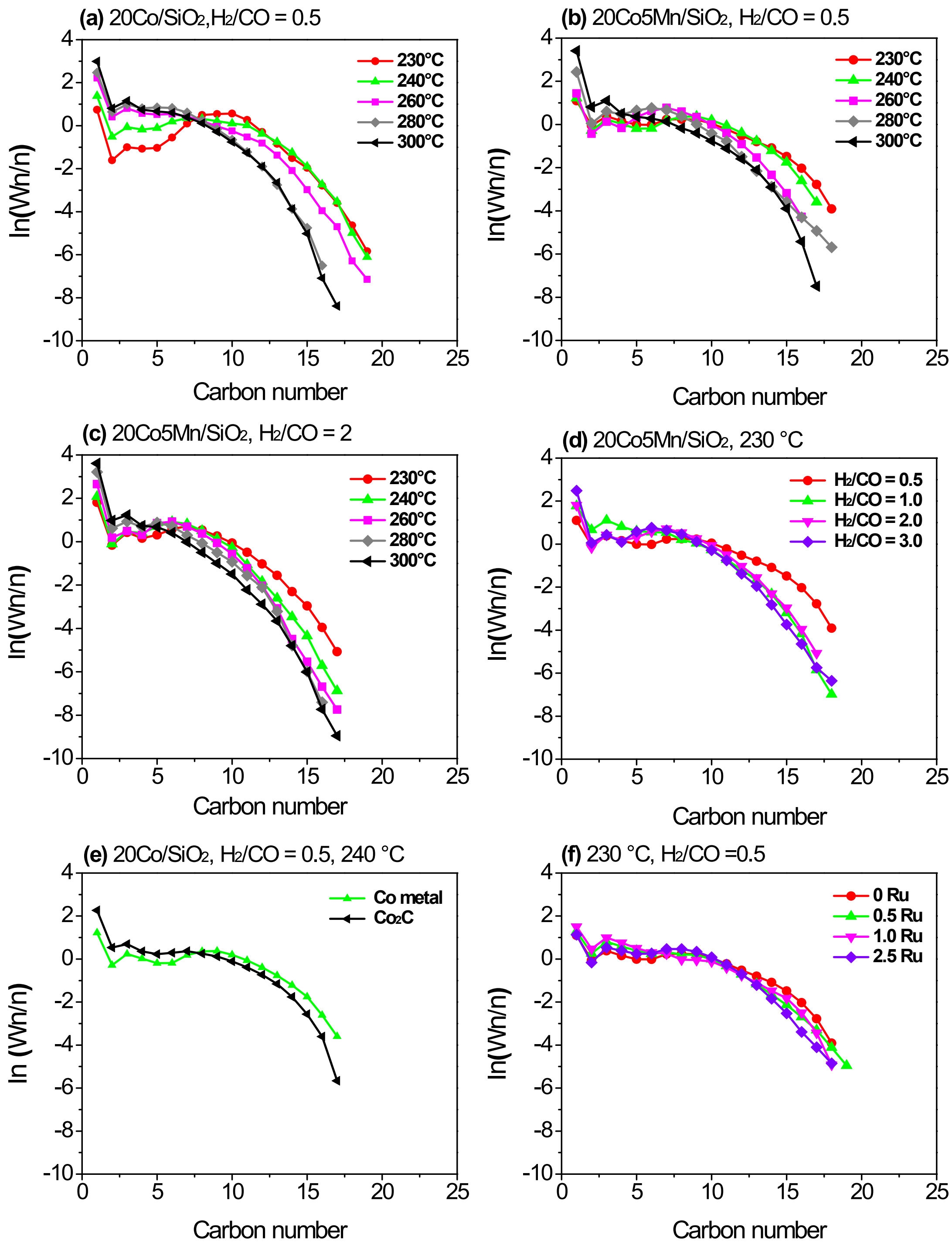

Figure S7 ASF plots of the FTS products under different catalysts and reaction conditions: (a) corresponding to product distribution in Fig. 7; (b) for that in Fig. 10; (c) for that in Fig. 11; (d) for that in Fig. 12; (e) for that in Fig. 13; (f) for that in Fig. S3.

Table S1 Influence of Ru loading on the catalytic performance over $20Co5Mn/SiO_2$ at H_2/CO = 0.5

Ru loading (wt%)	CO conversion (%)	Selectivity to CO_2 (%)	Hydrocarbon selectivity (%)				Total α-olefin (%)
			CH_4	$C_2^=$-$C_4^=$	C_2^0-C_4^0	C_{5+}	
0	4.4	1.1	3.6	12.6	2.1	81.7	67.3
0.5	5.1	0.9	4.6	17.5	3.4	74.5	65.2
1.0	5.6	0.7	4.5	16.6	3.1	75.8	56.3
2.5	9.3	0.8	3.8	13.2	2.7	80.3	62.6

Reaction conditions: catalyst loading = 1.0 g, T = 230°C, P = 1.0 MPa, GHSV = 4.5 L g_{cat}^{-1} h^{-1}. The CO conversion and $C_2^=$-$C_4^=$ selectivity, and CH_4 selectivity with TOS were shown in Fig. S3 and Fig. S6f.

Table S2 Influence of Co phase state on the catalytic performance over $20Co/SiO_2$ at H_2/CO = 0.5

Reaction temperature (°C) and TOS (h)	Co phase state	CO conversion (%)	Selectivity to CO_2 (%)	Hydrocarbon selectivity (%)				Total α-olefin (%)
				CH_4	$C_2^=$-$C_4^=$	C_2^0-C_4^0	C_{5+}	
300 (0-24)	Co_2C	54.4	40.7	21.8	12.1	9.6	56.5	30.7
240 (25-48)	Co_2C	13.7	20.6	9.6	10.6	4.2	75.6	37.0
240 (0-24)	Metallic Co	13.9	1.9	4.0	6.0	0.9	89.2	61.8

Reaction conditions: catalyst loading = 1.0 g, P = 1.0 MPa, GHSV = 4.5 L g_{cat}^{-1} h^{-1}. The CO conversion and $C_2^=$-$C_4^=$ selectivity, and CH_4 selectivity with TOS were shown in Fig. 13 and Fig. S6e.